

Spectroscopic and structural studies on 1:2 adducts of silver(I) salts with tricyclohexylphosphine*

Graham A. Bowmaker,^a Effendy,^{b,c} Peta J. Harvey,^d Peter C. Healy,^d Brian W. Skelton^b and Allan H. White^b

^a Department of Chemistry, University of Auckland, Private Bag 92019, Auckland, New Zealand

^b Department of Chemistry, University of Western Australia, Nedlands, Western Australia 6907, Australia

^c Jurusan Pendidikan Kimia, FPMIPA IKIP Malang, Jalan Surabaya 6, Malang 65145, Indonesia

^d Faculty of Science and Technology, Griffith University, Brisbane, Queensland 4111, Australia

A series of monomeric $[\text{AgX}\{\text{P}(\text{C}_6\text{H}_{11})_3\}_2]$ complexes have been prepared for X = CN, I, Br, Cl, SCN, NCO, NO₃ or ClO₄ and characterized by single-crystal X-ray determinations, solid-state cross polarization magic angle spinning (CP MAS) ³¹P NMR, solution ³¹P NMR and far-infrared spectroscopy. For X = CN, I, Br, Cl or SCN the crystal structures are isomorphous, crystallizing in a monoclinic C2/c cell with $a \approx 17$, $b \approx 9.3$, $c \approx 25$ Å, $\beta \approx 110^\circ$, $Z = 4$; the SCN complex exhibits anion disorder/space group ambiguity. For X = NCO or NO₃ (redetermined) the structures are isomorphous with the previously studied perchlorate, crystallizing in a triclinic P $\bar{1}$ cell derivative of the C2/c array with $a \approx 9.3$, $b \approx 9.8$, $c \approx 23$ Å, $\alpha \approx 95$, $\beta \approx 96$, $\gamma \approx 116^\circ$. The Ag–P bond lengths correlate inversely with the P–Ag–P angles and depend on the donor properties of the anion X, with, however, a reverse trend noted for the halide complexes. The solid-state CP MAS ³¹P NMR spectra show splitting due to ¹J(P–Ag) coupling which progressively increases from 322 Hz for X = CN to 505 Hz for X = ClO₄. For the triclinic species further splitting is observed and assigned to ²J(P–P) coupling between the crystallographically inequivalent phosphorus atoms. These NMR results are consistent with the structural results except for the chloride and perchlorate systems where experiments suggest that both triclinic and monoclinic phases co-crystallize in proportions which depend on the recrystallization procedures. Solution ³¹P NMR spectra show doublets assignable to 1:2 species. For X = Br, Cl, NCO or SCN signals assignable to 1:1 species are also observed. Comparison with solid-state data show differences in ¹J(P–Ag) that are ascribed to differences in $\theta(\text{P–Ag–P})$ in the solution and solid states. Far-IR spectra of the halide and pseudo-halide complexes in the series exhibit single bands due to $\nu(\text{AgX})$ vibrational modes at 207, 149, 121 for X = Cl, Br or I and at 288, 241 and 174 cm⁻¹ for X = CN, NCO or SCN, these latter results providing rare data for the vibrational frequencies of terminal Ag–C, Ag–N and Ag–S bonds.

Reaction of silver(I) salts with monodentate tertiary phosphines in a 1:2 stoichiometric ratio generally results in the formation of either monomeric $[\text{AgX}(\text{PR}_3)_2]/[\text{Ag}(\text{PR}_3)_2]^+ \text{X}^{-1-13}$ or dimeric complexes $[\{\text{AgX}(\text{PR}_3)_2\}_2]^{13-16}$ depending on the donor properties of the phosphine ligand, the bulkiness of the ligand substituents and the donor properties of the anion. The metal centre(s) in the majority of the neutral $[\text{AgX}(\text{PR}_3)_2]$ and $[\{\text{AgX}(\text{PR}_3)_2\}_2]$ complexes are predominantly four-co-ordinate with the anion acting as either a bidentate chelating ligand or as a bridging ligand with two- and three-co-ordination found only in circumstances where the anion is a weak donor and/or the substituents on the phosphine ligand are bulky.^{5,8,13} For example, with tricyclohexylphosphine, which is a basic tertiary phosphine ($\text{p}K_a = 9.65^{17}$) with relatively bulky substituents, mononuclear complexes of the type $[\text{AgX}\{\text{P}(\text{C}_6\text{H}_{11})_3\}_2]$ have been reported for X = ClO₄ or NO₃ in which the anion is bound to the metal through only one oxygen atom, making the silver atom three-co-ordinate.¹¹ We find that the analogous complexes for X = CN, I, Br, Cl, SCN or NCO similarly crystallize as monomers, providing a rare opportunity systematically to study an extended series of mononuclear $[\text{MXL}_2]$ species. We have obtained structural and spectroscopic information on these complexes in both the solution and solid

states through single-crystal X-ray crystallography, solid-state ³¹P NMR, solution ³¹P NMR and far-infrared spectroscopy and report the results of this work here.

Experimental

Synthesis

$[\text{AgX}\{\text{P}(\text{C}_6\text{H}_{11})_3\}_2]$ (X = Cl, Br, I, CN, SCN or NCO). Typically AgX (0.25–0.50 mmol) and P(C₆H₁₁)₃ (0.5–1.0 mmol) in a 1:2 stoichiometric ratio were dissolved in warm pyridine (5–10 cm³) to give clear solutions which on cooling and solvent evaporation deposited colourless crystals of the desired product. Compounds with X = NO₃ or ClO₄¹¹ were prepared similarly with ethanol as solvent for X = NO₃ and acetonitrile for X = ClO₄. X = Cl: m.p. > 148 °C (decomp.) (Found: C, 61.6; H, 9.6. C₃₆H₆₆AgClP₂ requires C, 61.40; H, 9.45%). X = Br: m.p. > 160 °C (decomp.) (Found: C, 58.0; H, 8.7. C₃₆H₆₆AgBrP₂ requires C, 57.75; H, 8.90%). X = I: m.p. > 169 °C (decomp.) (Found: C, 54.5; H, 8.4. C₃₆H₆₆AgIP₂ requires C, 54.35; H, 8.35%). X = CN: m.p. 155–157 °C (Found: C, 64.1; H, 9.3; N, 2.1. C₃₇H₆₆AgNP₂ requires C, 63.95; H, 9.55; N, 2.00%). X = SCN: m.p. 164–168 °C (Found: C, 61.3; H, 9.0; N, 2.1. C₃₇H₆₆AgNP₂S requires C, 61.15; H, 9.15; N, 1.95%). X = NCO: m.p. 216–218 °C (Found: C, 62.8; H, 9.1; N, 2.1. C₃₇H₆₆AgNOP₂ requires C, 62.50; H, 9.35; N, 1.95%).

* Non-SI unit employed: eV $\approx 1.60 \times 10^{-19}$ J.

Crystallography

Unique room-temperature diffractometer data sets (scan mode 2 θ - θ , monochromatic Mo-K α radiation, $\lambda = 0.71073$ Å) were measured yielding N independent reflections, N_o , with $I > 3\sigma(I)$ being considered 'observed' and used in the full-matrix least-squares refinements after analytical absorption corrections. Anisotropic thermal parameters were refined for the non-hydrogen atoms, $(x, y, z, U_{iso})_H$ being included constrained at estimated values. Conventional residuals on $|F|$, R and R' are quoted, statistical reflection weights being derivative of $\sigma^2(I_{diff}) = \sigma^2(I) + 0.0004\sigma^4(I_{diff})$. Neutral atom complex scattering factors were employed; computation used the XTAL 3.2 program system implemented by S. R. Hall.¹⁸ Abnormal features/variations in procedures/comments for individual samples are recorded below. In all figures 20% thermal ellipsoids are shown for the non-hydrogen atoms; hydrogen atoms, where included, have arbitrary radii of 0.1 Å. Ring carbon atoms are labelled C(lmm) (l = ligand number, m = ring number, n = atom number).

Crystal/refinement data. [AgCl{P(C₆H₁₁)₃}₂], C₃₆H₆₆AgClP₂, $M = 704.2$, monoclinic, space group C2/c (C_{2h}^6 , no. 15), $a = 16.881(4)$, $b = 9.199(4)$, $c = 24.604(7)$ Å, $\beta = 109.36(2)^\circ$, $U = 3605$ Å³, D_c ($Z = 4$) = 1.30 g cm⁻³; $F(000) = 1504$, $\mu_{Mo} = 6.7$ cm⁻¹, specimen 0.49 × 0.30 × 0.15 mm, $A^*_{min,max} = 1.10, 1.23$, $2\theta_{max} = 60^\circ$, $N = 4048$, $N_o = 3373$, $R = 0.026$, $R' = 0.029$.

[AgBr{P(C₆H₁₁)₃}₂], C₃₆H₆₆AgBrP₂, $M = 748.7$, monoclinic, space group C2/c, $a = 16.899(3)$, $b = 9.221(3)$, $c = 24.671(1)$ Å, $\beta = 109.44(3)^\circ$, $U = 3625$ Å³, D_c ($Z = 4$) = 1.37 g cm⁻³; $F(000) = 1576$, $\mu_{Mo} = 16.8$ cm⁻¹, specimen 0.60 × 0.25 × 0.27 mm, $A^*_{min,max} = 1.44, 1.60$; $2\theta_{max} = 60^\circ$; $N = 4782$, $N_o = 3633$, $R = 0.032$, $R' = 0.035$.

[AgI{P(C₆H₁₁)₃}₂], C₃₆H₆₆AgIP₂, $M = 795.7$, monoclinic, space group C2/c, $a = 16.911(8)$, $b = 9.303(4)$, $c = 24.79(1)$ Å, $\beta = 109.68(5)^\circ$, $U = 3672$ Å³, D_c ($Z = 4$) = 1.44 g cm⁻³, $F(000) = 1648$, $\mu_{Mo} = 13.7$ cm⁻¹, specimen 0.50 × 0.29 × 0.25 mm, $A^*_{min,max} = 1.33, 1.46$, $2\theta_{max} = 60^\circ$, $N = 4744$, $N_o = 3400$, $R = 0.036$, $R' = 0.041$.

[Ag(CN){P(C₆H₁₁)₃}₂], C₃₇H₆₆AgNP₂, $M = 694.8$, monoclinic, space group C2/c, $a = 16.827(4)$, $b = 9.330(2)$, $c = 24.670(8)$ Å, $\beta = 110.38(2)^\circ$, $U = 3631$ Å³, D_c ($Z = 4$) = 1.27 g cm⁻³, $F(000) = 1488$, $\mu_{Mo} = 5.9$ cm⁻¹, specimen 0.35 × 0.26 × 0.03 mm, $A^*_{min,max} = 1.02, 1.14$, $2\theta_{max} = 50^\circ$, $N = 2843$, $N_o = 2329$, $R = 0.030$, $R' = 0.033$.

[Ag(SCN){P(C₆H₁₁)₃}₂], C₃₇H₆₆AgNP₂S, $M = 726.8$, monoclinic, space group C2/c, $a = 16.993(4)$, $b = 9.313(4)$, $c = 24.78(3)$ Å, $\beta = 109.11(5)^\circ$, $U = 3706$ Å³, D_c ($Z = 4$) = 1.30 g cm⁻³, $F(000) = 1552$, $\mu_{Mo} = 6.3$ cm⁻¹, specimen 0.35 × 0.30 × 0.25 mm, $A^*_{min,max} = 1.14, 1.19$, $2\theta_{max} = 60^\circ$, $N = 5148$, $N_o = 3286$, $R = 0.051$, $R' = 0.052$.

The parameters $(x, y, z, U_{iso})_H$ were refined for all five structures. Atoms C, N of the cyanide were assigned on the basis of refinement behaviour. The thiocyanate ligand lies off-axis and was modelled as disordered; attempted refinement in lower symmetry (Cc) was unfruitful. The alternative C2/c settings are not dissimilar in dimensions [$c/\text{Å}$, $\beta/^\circ$ = 24.798(7), 110.60(2) (Cl); 24.84(1), 110.47(5) (Br); 24.86(1), 110.15(5) (I); 24.548(8), 109.60(2) (CN); 25.04(3), 110.77(5) (SCN)] and potential users should be aware of this alternative, as also of derivative triclinic arrays (see below).

[Ag(NCO){P(C₆H₁₁)₃}₂], C₃₇H₆₆AgNOP₂, $M = 710.8$, triclinic, space group $P\bar{1}$ (C_1^1 , no. 2), $a = 9.357(4)$, $b = 9.742(6)$, $c = 23.222(5)$ Å, $\alpha = 95.17(2)$, $\beta = 96.70(2)$, $\gamma = 116.97(4)^\circ$, $U = 1849$ Å³, D_c ($Z = 2$) = 1.28 g cm⁻³, $F(000) = 760$, $\mu_{Mo} = 6.6$ cm⁻¹, specimen 0.10 × 0.40 × 0.42 mm, $A^*_{min,max} = 1.07, 1.25$, $2\theta_{max} = 50^\circ$, $N = 6494$, $N_o = 5298$, $R = 0.035$, $R' = 0.041$.

[Ag(NO₃){P(C₆H₁₁)₃}₂], C₃₇H₆₆AgNO₃P₂, $M = 730.8$,

triclinic, space group $P\bar{1}$, $a = 9.263(5)$, $b = 9.819(10)$, $c = 23.403(6)$ Å, $\alpha = 94.67(5)$, $\beta = 96.45(3)$, $\gamma = 116.30(6)^\circ$, $U = 1876$ Å³, D_c ($Z = 2$) = 1.29 g cm⁻³, $F(000) = 780$, $\mu_{Mo} = 5.8$ cm⁻¹, specimen 0.03 × 0.34 × 0.25 mm, $A^*_{min,max} = 1.02, 1.12$, $2\theta_{max} = 50^\circ$; $N = 6580$, $N_o = 3799$; $R = 0.055$, $R' = 0.052$.

These latter two compounds were modelled as isomorphous in space group $P\bar{1}$ in a cell derivative of the foregoing C2/c array (Fig. 1). The cyanate was modelled as N-bound on the basis of refinement behaviour and associated geometry. Our observation of disorder in one of the cyclohexyl rings (21n) of the ligand in the cyanate is paralleled by the deconvolution of similar disorder in the nitrate structure, the disorder being modelled in terms of atomic fragments of equal population after trial refinement and possibly contributing to the somewhat better precision of the present nitrate determination *vis-à-vis* the previous;¹¹ the latter forms the basis of the present setting, but atoms have been relabelled to conform more closely to the C2/c array. In the course of our studies we also examined the perchlorate analogue which had been previously determined in company with the nitrate, but 'not isomorphous though the

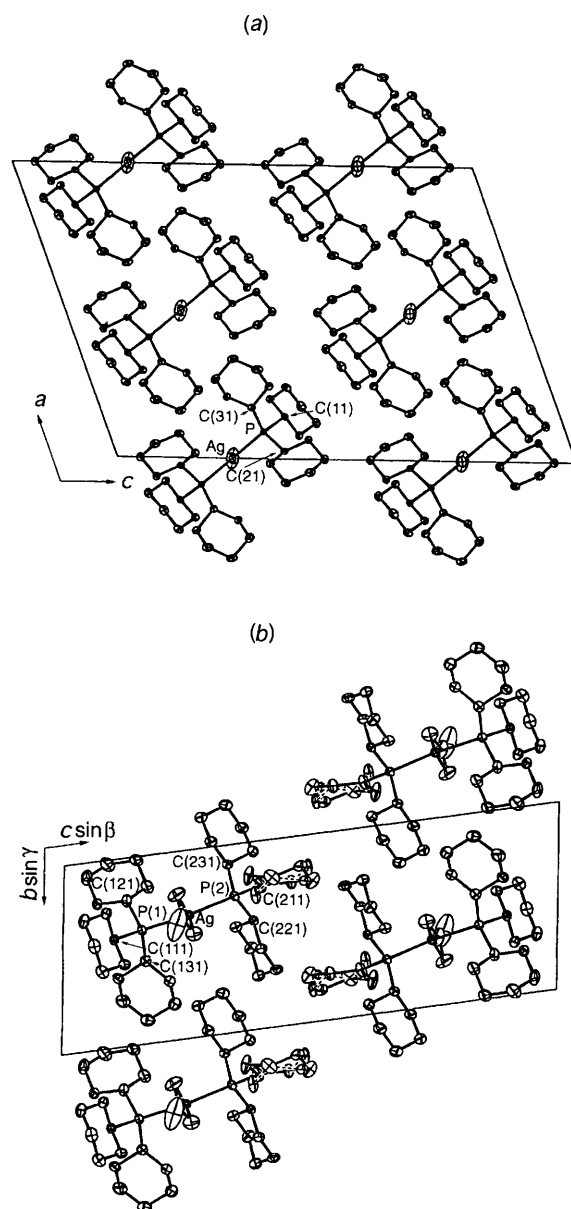


Fig. 1 (a) A typical unit for the C2/c phase cell projected down b (the cyanide). (b) A typical unit cell for the $P\bar{1}$ phase (the nitrate) projected down a

atomic z coordinates show some similarity'. We find it possible to transform the perchlorate cell and coordinates of ref. 11 into compatibility with those of the nitrate by adoption of a cell $a, b, c = 9.505(2), 9.790(2), 23.440(6)$ Å, $\alpha = 94.68(2)$, $\beta = 97.29(2)$, $\gamma = 115.97(1)^\circ$, *via* $a' = a$, $b' = b$ and new c as the old cell diagonal [previous: $c, \alpha, \beta, \gamma 23.667(6)$ Å, $99.03(2), 95.44(2), 115.97(1)^\circ$]; no disorder was recorded in either structure in the earlier study. In our own studies on the perchlorate the specimens prepared yielded a cell paralleling the above $C2/c$ dimensions with angles of 90° achievable with some specimens and appreciably divergent with others. Data refined on a $C2/c$ model on the specimen with $\alpha = \gamma = 90^\circ$ yielded a high residual which was little improved on adopting a triclinic model with a full hemisphere of data, and this remains essentially an 'unsolved' structure. These results are consistent with solid-state ^{31}P cross polarization magic angle spinning (CP MAS) NMR spectroscopic results which consistently show overlapping signals assignable to both monoclinic and triclinic phases on specimens of this complex (see Discussion). Multiphase/twinning behaviour in these complexes is consistent with the similarity in the unit-cell dimensions and the possibility remains that under varying recrystallization conditions examples of both structural types for each anion can be isolated. Overlapping CP MAS solid-state NMR signals assignable to species with one and two crystallographically independent phosphorus atoms were also observed for specimens of the chloride complex. However, our attempts to obtain untwinned triclinic crystals of this complex have not proven successful to date.

Atomic coordinates, thermal parameters and bond lengths and angles have been deposited at the Cambridge Crystallographic Data Centre (CCDC). See Instructions for Authors, *J. Chem. Soc., Dalton Trans.*, 1996, Issue 1. Any request to the CCDC for this material should quote the full literature citation and the reference number 186/41.

Spectroscopy

Solid-state CP MAS ^{31}P NMR spectra were obtained at ambient temperature on a Varian Unity-400 spectrometer at 161.92 MHz. Single contact times of 2 ms were used with a proton pulse width of 7.0 μs , a proton decoupling field of 62 kHz and a recycle delay time of 20 s. The samples were packed in Kel-F inserts within silicon nitride rotors and spun at a speed of 5 kHz at the magic angle. Between 60 and 200 free induction decays were collected and transformed with experimental line-broadening values of 10–20 Hz. Chemical shift data are referenced to 85% H_3PO_4 *via* an external sample of solid PPh_3 ($\delta -9.9$). On this scale, $\delta[\text{P}(\text{C}_6\text{H}_{11})_3]_{\text{solid}}$ is 6.8. Solution ^{31}P NMR spectra were recorded on the same instrument on saturated solutions in 3 cm^3 CDCl_3 or CH_2Cl_2 10% CD_2Cl_2 in 10 mm NMR tubes at variable temperatures (25 to -88°C). Spectra consisting of 8000 data points were acquired using an 8 μs (45°) pulse, proton-waltz decoupling and a 1 s relaxation delay. A total of 256 scans were collected and the spectra processed with 2 Hz line broadening. The chemical shifts were referenced to external 85% H_3PO_4 at $\delta 0$. Infrared spectra were recorded at 4 cm^{-1} resolution at room temperature as Nujol mulls between KBr plates on a Digilab FTS-60 Fourier-transform spectrometer employing an uncooled deuterated triglycine sulfate detector. Far-IR spectra were recorded at 4 cm^{-1} resolution at room temperature as pressed Polythene discs on a Digilab FTS-60 Fourier-transform spectrometer employing an FTS-60V vacuum optical bench with a 6.25 μm mylar-film beam splitter, a mercury lamp source and a triglycine sulfate detector. Raman spectra were excited with 100 mW of 514.5 nm radiation using a Coherent model 52 argon-ion laser and were recorded at 4.5 cm^{-1} resolution using a Jobin-Yvon U1000 spectrometer.

Results and Discussion

Structural data

The results of the present room-temperature single-crystal X-ray studies are consistent with the formulation of all the complexes as monomeric $[\text{AgX}\{\text{P}(\text{C}_6\text{H}_{11})_3\}_2]$ species. Taking into account the reservations concerning the thiocyanate noted above, the compounds with $\text{X} = \text{CN}, \text{I}, \text{Br}, \text{Cl}$ or SCN have been obtained in the monoclinic $C2/c$ lattice; four molecules are found in the unit cell, the individual molecules being disposed with crystallographic 2 axes lying between the ligands and coincident with the $\text{Ag}-\text{X}$ bonds, except for the thiocyanate, so that one half of the molecule is the asymmetric unit in each case [Fig. 2(a), (b)]. In these adducts, ring 1 from each ligand is located *cis* to the $\text{Ag}-\text{X}$ vector and lies approximately normal to the P_2AgX plane, the two rings forming a 'pocket' occupied by the anion. Non-bonding $\text{X}\cdots\text{H}$ contact distances between the anion atoms and the ring 1 hydrogens are all greater than 3.0 Å. Rings 2 and 3 are disposed *trans* to $\text{Ag}-\text{X}$ and lie above and below the P_2AgX plane. Ring 3 on each ligand is oriented towards the anions on adjacent molecules in the crystal lattice [Fig. 1(a)] with the shortest $\text{H}\cdots\text{X}$ non-contact distances of the order of 3.6 Å. All the closest hydrogen-hydrogen intra-ligand, intra- and inter-molecular contact distances between cyclohexyl rings lie at comfortable van der Waals distances.

The $\text{X} = \text{ClO}_4, \text{NO}_3$ or NCO complexes are obtained in a triclinic cell derivative of the above $C2/c$ array in which the two ligands are crystallographically independent and characterized by differences in conformational structure [Figs. 1(b), 2(c)]. The conformation of ligand 1 is essentially the same as that of both ligands in the $C2/c$ complexes. In ligand 2 ring (23*n*) adopts the same conformation as ring 3 in the $C2/c$ array while rings (21*n*) and (22*n*) are rotated by $\approx 90^\circ$ about their respective P-C bonds [Figs. 1(b), 2(c)] when compared to those in ligand 1. Ring (21*n*) is disordered and lies approximately parallel to the P_2AgX plane [Fig. 2(c)]. The $\text{H}(216a)\cdots\text{X}$ distances decrease to 2.8–2.9 Å, similar to those observed for the analogous triphenylphosphine/nitrate complex where phenyl ring 1 is oriented similarly.¹ Intermolecular packing in this triclinic cell is such that ligands with the same conformational structure are adjacent to each other [Fig. 1(b)].

The three-co-ordinate (P_2AgX) silver environment is necessarily planar for the $C2/c$ family of structures and is planar also for the triclinic cyanate structure with the sum of the N-Ag-P and P-Ag-P angles 359.8° . For the oxyanion complexes, the nitrate and perchlorate anions are potentially chelating and the metal four-co-ordinate as is observed for the analogous triphenylphosphine/nitrate complex.¹ However, as noted in the Introduction, for the present compounds one of the pair of nearest oxygen atoms is distinctly closer and, with the two phosphorus atoms, has an angle sum also not greatly removed from 360° (nitrate, 358.6 ; perchlorate, $356.3^{(1)}$). Geometric parameters for the AgXP_2 core geometries of these complexes are presented in Table 1, together with those of $[\text{AgBr}(\text{PPh}_3)_2]^{13}$ for comparison. The data for the $\text{P}(\text{C}_6\text{H}_{11})_3$ complexes show that the relationship between the Ag-P bond lengths and the P-Ag-P angles is quite complex (Fig. 3). While the longer Ag-P bond lengths are generally accompanied by smaller P-Ag-P angles, exceptions to this are found for the thiocyanate complex (where, however, the data should be considered circumspectly in the light of the disorder/structural ambiguity observed) and for the chloride, bromide and iodide complexes for which a reverse trend is noted. Correlation between increasing $d(\text{M}-\text{P})$ and decreasing $\theta(\text{P}-\text{M}-\text{P})$ has been noted previously for some silver(I) diphosphine complexes and for four-co-ordinate triphenylphosphine mercury(II) complexes, $[\text{HgX}_2(\text{PPh}_3)_2]$, where it is postulated that the magnitudes of both $d(\text{M}-\text{P})$ and $\theta(\text{P}-\text{M}-\text{P})$ are determined by the donor properties of the anion X as a result of competition for electron

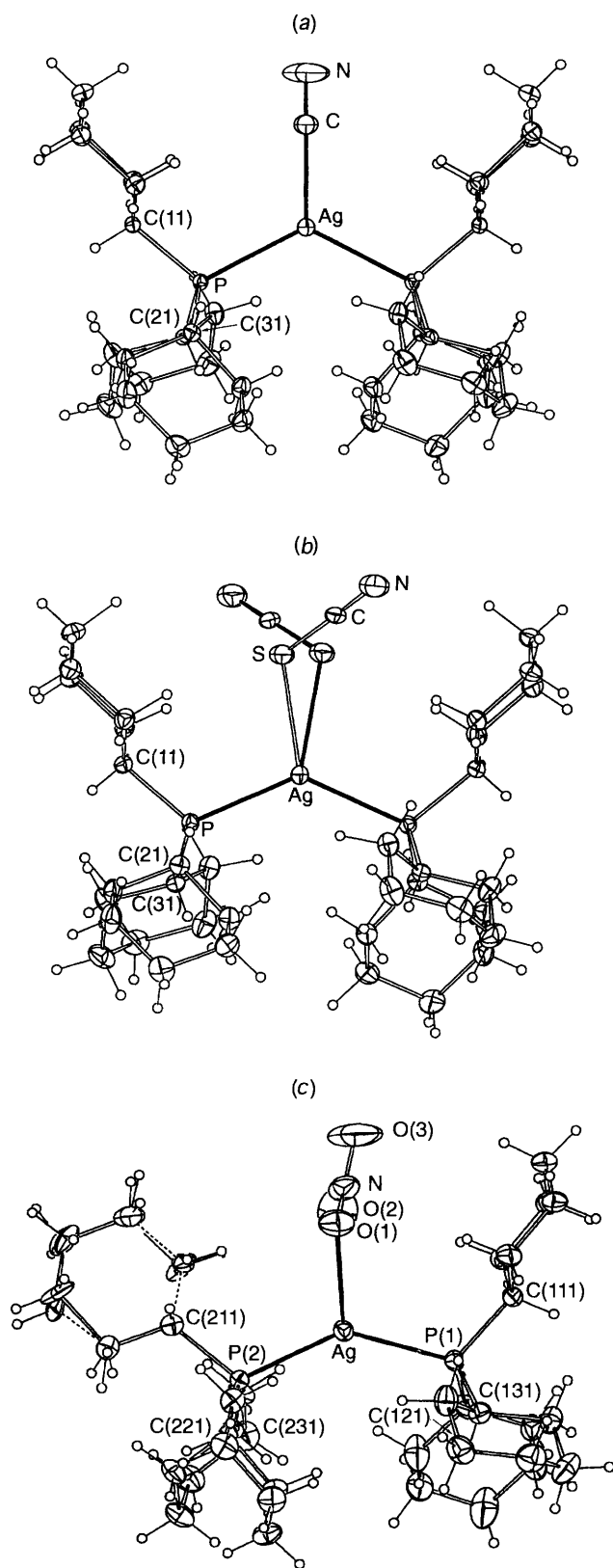


Fig. 2 Crystal structures of (a) the cyanide, (b) the thiocyanate (with disordered SCN) and (c) the nitrate, showing the reoriented ligand (with disorder), projected normal to the AgP_2 plane

density between the M-P and M-X bonds.¹⁹⁻²¹ If M-X bonding were non-existent, as in ionic $[\text{M}(\text{PR}_3)_2]^+ \text{X}^-$, then the P-M-P angle in the isolated cation would be 180° . For a given phosphine, as the M-X bond strength increases, the P-M-P angle decreases and the M-P bond length correspondingly is expected to increase as a consequence of decreasing M-P bond strength but also, for bulky phosphines, from increased steric

Table 1 Molecular core geometries for monomeric $[\text{AgX}\{\text{P}(\text{C}_6\text{H}_{11})_3\}_2]$ complexes

X	$d(\text{Ag-P})/\text{\AA}$	$d(\text{Ag-X})/\text{\AA}$	$\theta(\text{P-Ag-P})/^\circ$	$\theta(\text{P-Ag-X})/^\circ$
CN	2.4803(9)	2.153(6)	124.86(4)	117.57(2)
I	2.478(1)	2.778(1)	130.75(4)	114.62(3)
Br	2.4734(9)	2.618(1)	129.42(3)	115.29(2)
Cl	2.4712(8)	2.489(1)	128.29(3)	115.85(2)
SCN	2.486(2)	2.572(3)	131.51(7)	123.69(8)
			104.60(8)	
NCO	2.457(1)	2.205(6)	133.65(4)	111.6(1)
	2.454(1)			114.5(1)
NO_3	2.451(2)	2.47(1)	139.14(9)	110.5(2)
	2.440(2)	2.79(1)		109.0(2)
ClO_4	2.429(1)	2.720(7)	147.34(3)	98.5(1)
	2.4323(9)	3.014(9)		113.5(1)
Br*	2.458(2)	2.568(1)	124.14(5)	117.93(3)

For the cyanide C-N 1.029(9) Å; for the thiocyanate C-S 1.60(1), C-N 1.15(2) Å, S...S' 0.965(8) Å; for the cyanate C-N 1.06(1), N-O 1.25(1) Å, Ag-N-C 151.2(5), N-C-O 174.5(6)°. Data for $[\text{Ag}(\text{ClO}_4)\{\text{P}(\text{C}_6\text{H}_{11})_3\}_2]$ is taken from ref. 7 and $[\text{AgBr}(\text{PPh}_3)_2]$ from ref. 13. * $[\text{AgBr}(\text{PPh}_3)_2]$.

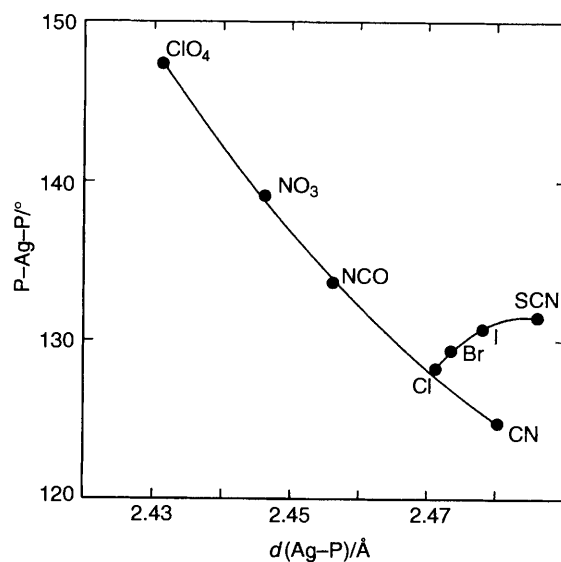


Fig. 3 The $d(\text{Ag-P})$ vs. $\theta(\text{P-Ag-P})$ correlation for $[\text{AgX}\{\text{P}(\text{C}_6\text{H}_{11})_3\}_2]$

crowding as the ligand substituents move closer together. This is analogous to the *trans* influence in two-co-ordinate linear or four-co-ordinate square-planar complexes where the properties of a particular bond, such as its length, can be affected by the nature of the bond which is *trans* to it. In the case of a three-co-ordinate trigonal complex $[\text{MXL}_2]$ the effect of the change is most notable in the L-M-L angle. This mode of co-ordination is relatively rare and it is even more unusual to find an extensive isostructural series of such complexes in circumstances uncomplicated by factors such as variable crystal lattice or solvent interactions. The present results show that the bond-angle changes in this situation are quite sensitive to changes in the nature of X, the angle decreasing from $147.34(3)^\circ$ for X = ClO_4 to $124.86(4)^\circ$ for X = CN. Along the series X = Cl, Br, I, however, the P-Ag-P angle increases rather than decreases (as might be expected on the basis of the expected relative donor strengths of the three anions) implying that either the Ag-Cl interaction is the strongest in the halide series or that even in this series of isostructural complexes the magnitude of $\theta(\text{P-Ag-P})$ can be affected by steric as well as covalent bonding interactions. This point is discussed further below in the context of the solution and solid-state ^{31}P NMR results, but we note here that an expectation that the donor strength of the Cl, Br and I complexes increases significantly from chloride to iodide

may not always be valid. Trends in Ag–X bond strengths as reflected in the dissociation energies of diatomic AgX (3.22, 3.1, 2.6 eV for X = Cl, Br and I respectively)²² suggest that the Ag–Cl bond may be the strongest in this situation while calculations carried out on similar systems provide a bonding description in which the metal p orbitals contract to a greater extent for the small halide anions to allow stronger metal–halide bonding interactions and where the extent of halide ligand-to-metal charge transfer is very similar for the different halides.^{23, 24}

Direct comparison of these results with other analogous three-co-ordinate complexes is presently very limited with data only available for [AgBr(PPh₃)₂] and [AgBr{P(C₆H₁₁)₃}₂] complexes where *d*(Ag–Br), θ (P–Ag–P) and *d*(Ag–P) are each greater in the P(C₆H₁₁)₃ complex. The increase in *d*(Ag–Br) and θ (P–Ag–P) is consistent with the greater σ -donor strength of P(C₆H₁₁)₃ resulting in [P(C₆H₁₁)₃}₂⁺ acting as a relatively weaker acceptor for the bromide anion (see also the vibrational spectroscopic results below); however, it might be expected that this also would lead to a decrease in *d*(Ag–P). That an increase is observed instead may be a reflection of the greater steric bulk of the cyclohexyl rings in P(C₆H₁₁)₃ by comparison with the phenyl rings in PPh₃. Recent studies²⁵ also suggest that the M–P bond length does not necessarily correlate with bond strength when there is a change in the nature of the phosphine ligand.

Infrared spectroscopy

The far-IR spectra of [AgX{P(C₆H₁₁)₃}₂] for X = halide and pseudo-halide are shown in Figs. 4 and 5. Uncomplexed P(C₆H₁₁)₃ shows no bands of significant intensity below 370 cm⁻¹. The spectra of the complexes show bands above 370 cm⁻¹ which are almost identical in wavenumber to bands in the spectrum of P(C₆H₁₁)₃, and these are assigned to the co-ordinated phosphine. Single bands, the wavenumbers of which are strongly dependent on the nature of X, were observed in the region below 250 cm⁻¹, and these are assigned to the ν (AgX) modes. The wavenumbers of these bands are compared in Table 2 with those of some related complexes. Comparison of ν (AgBr) for [AgBr{P(C₆H₁₁)₃}₂] with that of the corresponding PPh₃ complex reveals a significant increase in going from the P(C₆H₁₁)₃ to the PPh₃ complex and is consistent with the longer Ag–Br bond length found for the former.

While there have been several vibrational spectroscopic studies of silver thiocyanate systems,^{26, 27} there have been no definitive assignments of the silver–thiocyanate bond-stretching mode. The discovery in this work of the unusual [Ag(SCN){P(C₆H₁₁)₃}₂] complex which contains a single terminal SCN group provides an opportunity to observe this mode. The weak band at 174 cm⁻¹ seems to occur at the correct position to allow assignment as ν (AgS) of the silver–thiocyanate bond. While there are no previous assignments for silver(I) complexes, there are some for gold(I) thiocyanate compounds which allow a comparison. Thus, it has been shown that the ν (AuS) modes in [Au(SCN)₂]⁻ occur at wavenumbers which lie between those of the corresponding chloride and bromide complexes.^{30–32} An analogous situation is observed for the ν (AgS) assignment made here (Table 2). The intensity of this band in the IR spectrum is significantly less than those of the ν (AgX) modes in the halide complexes (Fig. 4) and this suggests a possible reason why bands due to this mode have not been observed previously for other Ag(SCN) complexes. The ν (CN) wavenumber in the IR spectrum is identical to that for [Ag(SCN)₂]⁻ (Table 2).

The ν (AgC) wavenumber for [Ag(CN){P(C₆H₁₁)₃}₂] is compared in Table 2 with the values for the [Ag(CN)₂]⁻ species.²⁸ It is clear that there is a considerable reduction in the wavenumber of this mode from the two- to the three-co-ordinate complex, and this parallels earlier findings on the

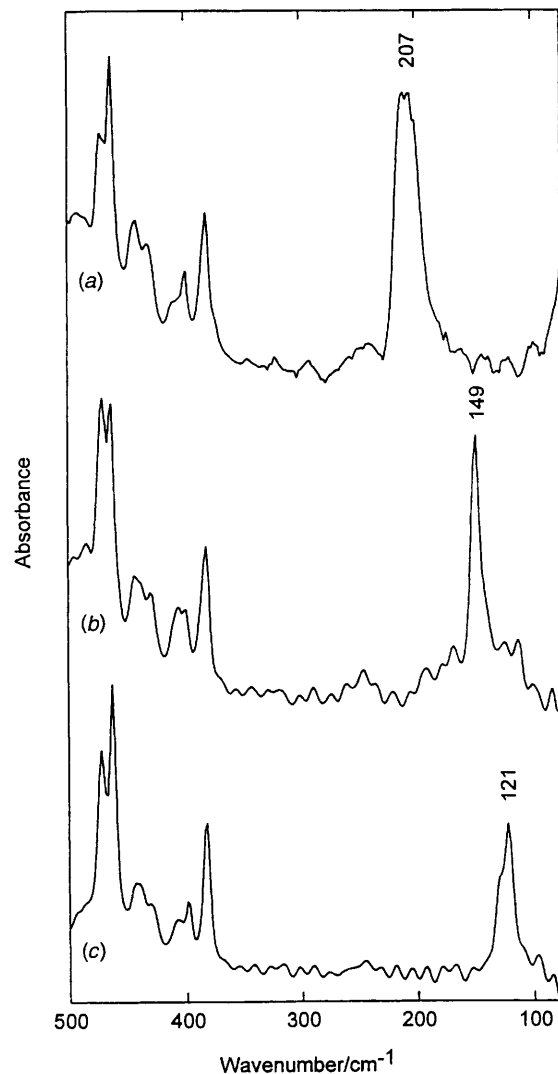


Fig. 4 Far-IR spectra of [AgX{P(C₆H₁₁)₃}₂]: X = Cl (a), Br (b) or I (c). The bands assigned to the ν (AgX) modes are labelled with their wavenumbers

behaviour of the analogous halide complexes.³³ The ν (CN) wavenumber lies between the values observed for the free cyanide ion (2080 cm⁻¹) and [Ag(CN)₂]⁻ (ca. 2140 cm⁻¹, Table 2). The cyanide ion may behave as a σ -donor and as a π -acceptor ligand; σ donation results in an increase in ν (CN), whereas π acceptance has the reverse effect.²⁹ Since CN⁻ is a better σ donor than π acceptor, ν (CN) is normally higher than that of free CN⁻, as is observed in the present case. The fact that the increase is less than in [Ag(CN)₂]⁻ indicates that in the present three-co-ordinate complex the cyanide ligand is not able to donate as much σ -electron density as in the two-co-ordinate [Ag(CN)₂]⁻. This results in a weaker Ag–C bond, and this fits in well with the explanation for the relatively low ν (AgC) values discussed above.

The ν (AgN) wavenumber for [Ag(NCO){P(C₆H₁₁)₃}₂] is compared in Table 2 with the values for [Ag(NCO)₂]⁻.²⁷ As in the case of the corresponding cyanide complexes discussed above, there is a considerable reduction in the frequency of this mode from the two- to the three-co-ordinate complex. It has been claimed that ν (CO) increases relative to the free-ion value (ca. 1250 cm⁻¹)²⁹ upon N-co-ordination,²⁷ and this is observed in the present complex, supporting the assignment of N-co-ordination in the structural determination. The δ (NCO) mode is observed as a doublet at 615, 624 cm⁻¹, slightly below the wavenumber for the free cyanate ion (629 cm⁻¹).²⁹

Raman spectra were also recorded with the aim of

Table 2 Wavenumbers (cm^{-1}) for $[\text{AgX}\{\text{P}(\text{C}_6\text{H}_{11})_3\}_2]$ and related complexes*

Complex	$\nu(\text{AgX})$	$\nu(\text{CN})$	$\nu(\text{CO})$	Ref.
$[\text{AgCl}\{\text{P}(\text{C}_6\text{H}_{11})_3\}_2]$	207			This work
$[\text{AgBr}\{\text{P}(\text{C}_6\text{H}_{11})_3\}_2]$	149			This work
$[\text{AgI}\{\text{P}(\text{C}_6\text{H}_{11})_3\}_2]$	121			This work
$[\text{AgBr}(\text{PPh}_3)_2]$	170			13
$[\text{Ag}(\text{SCN})\{\text{P}(\text{C}_6\text{H}_{11})_3\}_2]$	174	2090		This work
$[\text{Ag}(\text{SCN})_2]^-$	—	2090 (IR) 2092 (R)		26
$[\text{Ag}(\text{CN})\{\text{P}(\text{C}_6\text{H}_{11})_3\}_2]$	288			This work
$\text{K}[\text{Ag}(\text{CN})_2]$	396 (IR) 360 (R)	2140 (IR) 2146 (R)		28
$[\text{Ag}(\text{NCO})\{\text{P}(\text{C}_6\text{H}_{11})_3\}_2]$	241	2166	1301	This work
$[\text{NMe}_4][\text{Ag}(\text{NCO})_2]$	390 (IR) 375 (R)	2142 (IR) 2218 (R)	1287 (IR) 1320 (R)	27

* $\nu(\text{CN})$ and $\nu(\text{CO})$ for the cyanate ligand are usually referred to as $\nu_{\text{asym}}(\text{NCO})$ and $\nu_{\text{sym}}(\text{NCO})$ respectively. IR = Infrared, R = Raman.

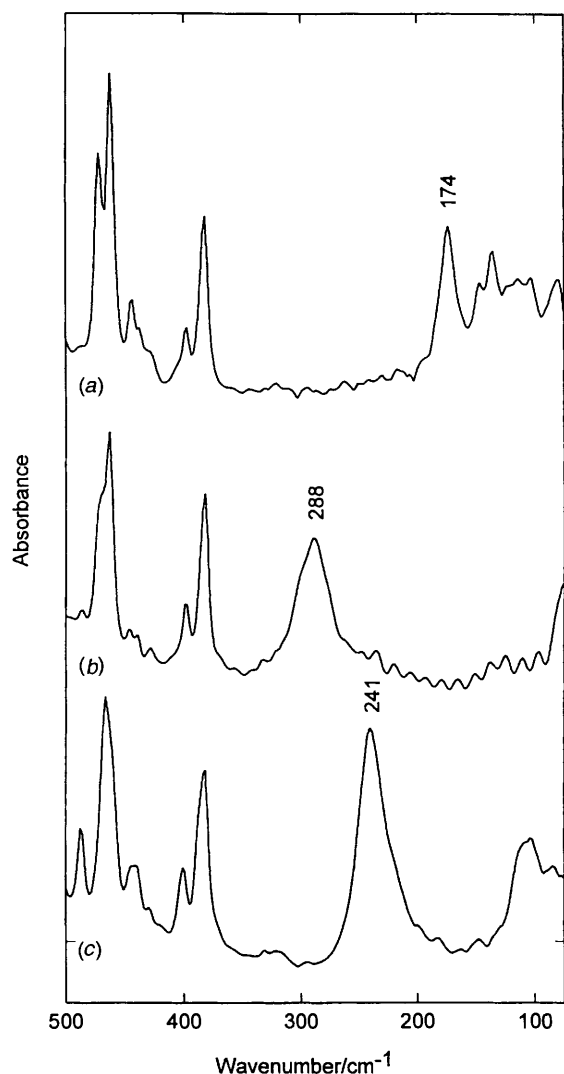


Fig. 5 Far-IR spectra of $[\text{AgX}\{\text{P}(\text{C}_6\text{H}_{11})_3\}_2]$: X = SCN (a), CN (b) or NCO (c). The bands assigned to the $\nu(\text{AgX})$ modes are labelled with their wavenumbers

determining the $\nu(\text{AgP})$ wavenumbers for the complexes. Previous Raman studies of $[\text{AgX}(\text{PPh}_3)_2]$ ($\text{M} = \text{Ag}$, $\text{X} = \text{Br}$; $\text{M} = \text{Au}$, $\text{X} = \text{Cl}$, Br or I) have resulted in the assignment of $\nu(\text{MP})$ bands.¹³ These bands are not visible in the IR spectra, probably due to the low polarity of the $\text{M}-\text{P}$ bonds. However, the Raman spectra of the present complexes were not of good quality and in most cases it was not even possible to detect the $\nu(\text{AgX})$ bands which were clearly evident in the far-IR spectra.

However, in the case of $[\text{AgBr}\{\text{P}(\text{C}_6\text{H}_{11})_3\}_2]$, the Raman spectrum showed weak bands at 133 and 149 cm^{-1} . The latter is assigned to $\nu(\text{AgBr})$, its wavenumber being identical to that of the corresponding band in the far-IR spectrum, and the former is assigned to $\nu(\text{AgP})$, its wavenumber being almost identical to that observed for the corresponding PPh_3 complex (132 cm^{-1}).

CP MAS ^{31}P NMR spectroscopy

The naturally occurring isotopes of silver (^{107}Ag , 51.82% natural abundance; ^{109}Ag , 48.18%) both have nuclear spin $I = \frac{1}{2}$, and their magnetogyric ratios are similar in magnitude [$\gamma(^{109}\text{Ag})/\gamma(^{107}\text{Ag}) = 1.15$]. Thus, the ^{31}P NMR spectra of complexes of silver(I) with phosphorus-donor ligands may show splitting due to $^1J(\text{P}-\text{Ag})$ coupling. Despite the existence of a large number of silver(I) complexes with phosphine ligands, relatively few solid-state ^{31}P NMR studies have been reported to date.^{1,2,6,13,34,35} These spectra normally show splitting due to $^1J(\text{P}-\text{Ag})$ coupling, but the separate splitting due to the ^{107}Ag and ^{109}Ag nuclei which is usually observed in solution studies is not normally resolved in the solid state due to the greater linewidths ($\Delta\nu \approx 40$ Hz) which are observed under these conditions.

The ^{31}P CP MAS NMR spectra of selected $[\text{AgX}\{\text{P}(\text{C}_6\text{H}_{11})_3\}_2]$ complexes are shown in Fig. 6 and chemical shift and coupling-constant data are listed in Table 3. For $\text{X} = \text{CN}$, I , Br or SCN , simple doublets are observed due to $^1J(\text{P}-\text{Ag})$ coupling arising from the A_2 part of an A_2X spin system, where A_2 represents the two crystallographically equivalent P nuclei and X the Ag nucleus, separation of the splitting due to the ^{107}Ag and ^{109}Ag nuclei not being resolved [Fig. 6(a)]. The NCO and NO_3 complexes give an eight-line spectrum due to the AM part of an AMX system in which the signals from two inequivalent phosphorus sites (A, M) are split into doublets from two potentially different $^1J(\text{P}-\text{Ag})$ couplings and then further split through smaller $^2J(\text{P}-\text{P})$ coupling between the two phosphorus atoms [Fig. 6(b)]. As noted earlier, experiments on the Cl and ClO_4 complexes show overlapping NMR signals that are a mixture of A_2X and AMX spin systems in proportions which depend on the recrystallization conditions and which are assigned to monoclinic and triclinic phases respectively [Fig. 6(c)]. The upfield signal in the spectra of the triclinic complexes matches that for the $\text{C}2/c$ species, and is assigned to the phosphorus atom P(1) with the downfield signal assigned to P(2). The $^1J(\text{P}-\text{Ag})$ values observed in the present study generally fit in well with the relationships between this parameter and molecular structure which have previously been observed for other $[\text{Ag}(\text{PR}_3)_2]^+$ systems.^{1,6,13,34,35} The compound most closely related to the present series in terms of molecular structure is three-co-ordinate $[\text{AgBr}(\text{PPh}_3)_2]$,¹³ and it is interesting that, despite the significant differences in both

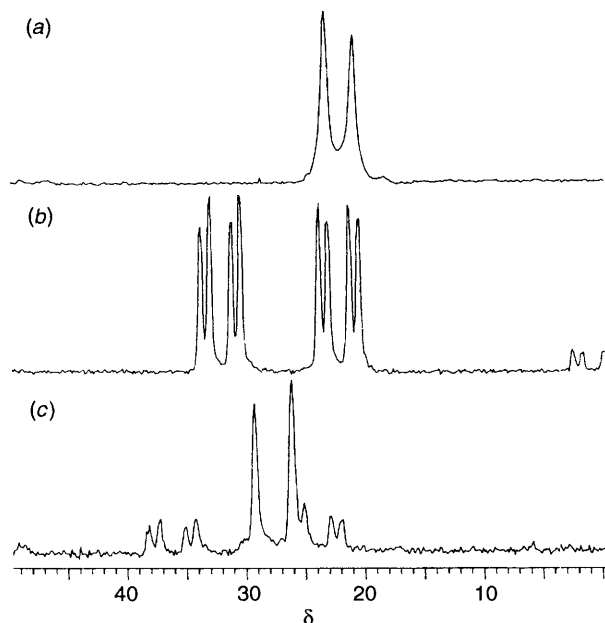


Fig. 6 Solid-state ^{31}P CP MAS NMR spectra of (a) $[\text{AgI}\{\text{P}(\text{C}_6\text{H}_{11})_3\}_2]$ (monoclinic), (b) $[\text{Ag}(\text{NCO})\{\text{P}(\text{C}_6\text{H}_{11})_3\}_2]$ (triclinic) and (c) $[\text{Ag}(\text{ClO}_4)\{\text{P}(\text{C}_6\text{H}_{11})_3\}_2]$ (mixture of monoclinic and triclinic forms)

$d(\text{Ag}-\text{P})$ and $\theta(\text{P}-\text{Ag}-\text{P})$, $^1J(\text{P}-\text{Ag})$ for the two complexes is the same within experimental error.

Changes in one-bond phosphorus–metal coupling constants have been interpreted in terms of a hybridization model^{19–21,36} based on the equation given by Pople and Santry³⁷ which assumes that changes in this constant $^1J(\text{P}-\text{M})$ are dominated by changes in the Fermi contact term, *via* equation (1), where

$$^1J(\text{P}-\text{M}) = \alpha_{\text{M}}^2 \alpha_{\text{P}}^2 (\Delta E)^{-1} |\psi_{\text{ns}}(0)_{\text{M}}|^2 |\psi_{3\text{s}}(0)_{\text{P}}|^2 \quad (1)$$

α_{M}^2 and α_{P}^2 are the s characters of the hybrid orbitals used to form the M–P bond, ΔE is the mean triplet excitation energy and $|\psi_{\text{ns}}(0)_{\text{M}}|^2$ and $|\psi_{3\text{s}}(0)_{\text{P}}|^2$ are the valence s-electron densities at the metal and phosphorus nuclei respectively. Assuming that the $|\psi_{\text{ns}}(0)|^2$ and ΔE terms do not change significantly for a related series of molecules, and that α_{P}^2 is constant for a given phosphine ligand,³⁶ the value of the coupling constant is determined by the metal s-orbital character α_{M}^2 . This parameter is determined by the metal–ligand bond angles *via* symmetry and orthogonality conditions and it is expected to increase as $\theta(\text{P}-\text{Ag}-\text{P})$ increases. Such a positive correlation between $\theta(\text{P}-\text{Ag}-\text{P})$ and solution-state $^1J(\text{P}-\text{Ag})$ data has been observed previously for silver(I) diphosphine and four-co-ordinate $[\text{HgX}_2(\text{PPh}_3)_2]$ complexes.^{19–21} The present study tests the validity of the hypothesis further by extending the range of anions under consideration and utilizing structural and spectroscopic data recorded in the solid state on the same sample for each compound. While the broad trends remain consistent with the model (Table 3, Fig. 7), the results for the three halide ligands ($\text{X} = \text{Cl}, \text{Br}$ or I) show that the value of $^1J(\text{P}-\text{Ag})$ for the iodide is only slightly less than those for the chloride and bromide which are the same within experimental error. This result is consistent with the notion discussed earlier that the donor strengths of the halide anions may be very similar in this type of complex. However, this does not provide an explanation of why $^1J(\text{P}-\text{Ag})$ does not follow the trend in $\theta(\text{P}-\text{Ag}-\text{P})$ for these complexes and the exact cause for this remains unknown. Nevertheless, the present study of the silver(I) systems provides the clearest evidence to date for this behaviour, and it is interesting that it does not occur for the

Table 3 The CP MAS ^{31}P NMR parameters for $[\text{AgX}\{\text{P}(\text{C}_6\text{H}_{11})_3\}_2]$ complexes (estimated error in coupling constants ± 10 Hz)

X	Phase	δ	$^1J(\text{P}-\text{Ag})/\text{Hz}$	$^2J(\text{P}-\text{P})/\text{Hz}$
CN	a	24.3	322	
I	a	22.1	386	
Br	a	22.3	396	
Cl	a	22.1	400	
Cl	b	21.8, 25.9	400, 410	120
SCN	a	28.6	404	
NCO	b	22.2, 32.1	415, 410	127
NO_3	b	25.0, 34.3	475, 470	132
ClO_4	a	27.8	505	
ClO_4	b	23.6, 36.8	500, 500	145
Br^c		6.0	394	

^a Monoclinic. ^b Triclinic. ^c Data for $[\text{AgBr}(\text{PPh}_3)_2]$ taken from ref. 13.

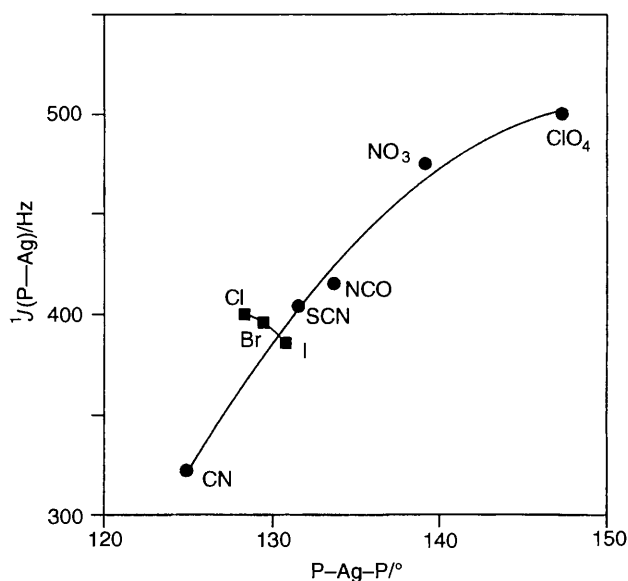


Fig. 7 The $^1J(\text{P}-\text{Ag})$ vs. $\theta(\text{P}-\text{Ag}-\text{P})$ correlation for $[\text{AgX}\{\text{P}(\text{C}_6\text{H}_{11})_3\}_2]$

pseudo-halide ligands which display the expected increase in $^1J(\text{P}-\text{Ag})$ with increasing $\theta(\text{P}-\text{Ag}-\text{P})$.

For those phases in which both phosphine ligands are crystallographically independent, $^2J(\text{P}-\text{P})$ is also obtainable from the solid-state ^{31}P NMR spectra, and the results are listed also in Table 3. It is evident that this parameter, too, shows an increase with increasing $\text{P}-\text{Ag}-\text{P}$ angle and this can be interpreted in a similar way to the discussion above for $^1J(\text{P}-\text{Ag})$.

Solution ^{31}P NMR studies

The solution and solid-state structures of transition-metal complexes are not necessarily the same and this is particularly likely to be the case in series of complexes where it is possible for several species to exist in solution, in varying degrees of aggregation through exchange equilibria. The $[\{\text{AgX}(\text{PR}_3)_m\}_n]$ complexes have been studied quite extensively in solution by ^{31}P NMR spectroscopy,^{6,34,35,38,40} with broad singlets being normally observed at ambient temperatures due to rapid exchange equilibria. However, at low temperatures exchange is stopped and typical pairs of doublets due to coupling of ^{31}P to both ^{107}Ag and ^{109}Ag are resolved. To investigate the structural characteristics of this present series of complexes in solution, we recorded variable-temperature solution ^{31}P NMR spectra in CDCl_3 and/or $\text{CD}_2\text{Cl}_2-\text{CH}_2\text{Cl}_2$ solutions, together with spectra of $[\text{AgBr}(\text{PPh}_3)_2]$ for comparative purposes. The results are presented in Table 4 with representative spectra shown in Fig. 8. Spectra of the $\text{X} = \text{ClO}_4$ and NO_3 complexes

Table 4 Solution ^{31}P NMR parameters for $[\text{AgX}\{\text{P}(\text{C}_6\text{H}_{11})_3\}_2]$ complexes (estimated error in coupling constants ± 5 Hz)

X	δ	$T/^\circ\text{C}$	$^1J/\text{Hz}$		
			$\text{P}-^{107}\text{Ag}$	$\text{P}-^{109}\text{Ag}$	$\text{P}-\text{Ag}$
CN	26.6	-88	327	378	352
I	26.9	-20	401	462	432
Br	28.4	-20	414	477	446
Cl	28.9	-20	415	479	447
SCN	31.7	0	407	469	438
NCO	29.2	-50	412	476	444
NO_3	32.8	+25	455	527	491
ClO_4	37.3	+25	462	534	498
Br^*	8.0	-88	—	—	420

* For $[\text{AgBr}(\text{PPh}_3)_2]$.

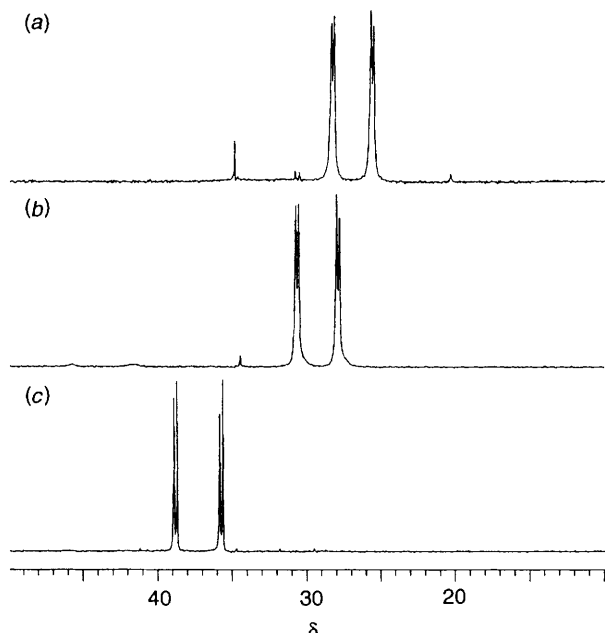


Fig. 8 Solution ^{31}P NMR spectra (CDCl_3) of (a) $[\text{AgI}\{\text{P}(\text{C}_6\text{H}_{11})_3\}_2]$ (-20°C), (b) $[\text{Ag}(\text{NCO})\{\text{P}(\text{C}_6\text{H}_{11})_3\}_2]$ (-50°C) and (c) $[\text{Ag}(\text{ClO}_4)\{\text{P}(\text{C}_6\text{H}_{11})_3\}_2]$ (25°C)

each show well resolved pairs of doublets at room temperature assignable to 1:2 species which is consistent with previously reported results.¹¹ Resolution of signals for 1:2 species for the other complexes required lower temperatures as recorded in Table 4. The results show that the chemical shifts for these species correspond reasonably well with the downfield signal observed in the solid-state spectra of the triclinic complexes. For $\text{X} = \text{Br}, \text{Cl}, \text{NCO}$ or SCN (but not for $\text{X} = \text{I}$) the spectra also show further downfield peaks assignable to 1:1 species on the basis of chemical shift and line spacing.⁴¹ By contrast, the spectrum of $[\text{AgBr}(\text{PPh}_3)_2]$ at -88°C shows a resolved doublet at $\delta 2$ with $^1J(\text{P}-\text{Ag}) = 290$ Hz assignable to the 1:3 species [cf. $^1J(\text{P}-\text{Ag}) = 300$ Hz for $[\text{AgBr}\{\text{P}(\text{C}_6\text{H}_4\text{Me-}p)_3\}_3]$ ³⁸] plus an unresolved doublet [$\delta 8$, $^1J(\text{P}-\text{Ag}) = 420$ Hz] assignable to the 1:2 species.

The effect of anion on the relative values of $^1J(\text{P}-\text{Ag})$ in the solution state is similar to that found in the solid state, with $^1J(\text{P}-\text{Ag})$ increasing with increasing donor strength of the anion. The reverse trend for the halides observed in the solid-state spectra is observed in the solution spectra as well, suggesting this effect is not due to solid-state intermolecular lattice interactions. The results also show that $^1J(\text{P}-\text{Ag})$ can differ significantly in the solid and solution states of a given complex. The largest differences observed are ca. 50 Hz for the three halides (the solution values being greater); for the pseudo-

halides ($\text{CN}, \text{SCN}, \text{NCO}$) this difference decreases to ca. 30 Hz, while for the nitrate and perchlorate complexes the differences are negligible. For comparison, the difference in $^1J(\text{P}-\text{Ag})$ for $[\text{AgBr}(\text{PPh}_3)_2]$ in solution and solid states is ca. 20 Hz. Given the observed dependence of $^1J(\text{P}-\text{Ag})$ on $\theta(\text{P}-\text{Ag}-\text{P})$, these results suggest that $\theta(\text{P}-\text{Ag}-\text{P})$ increases in solution for the halide and pseudo-halide complexes but not for the nitrate and perchlorate complexes. An increase in $\theta(\text{P}-\text{Ag}-\text{P})$ in solution is consistent with increased ligand-ligand interactions arising from greater mobility of the substituent rings and the small changes observed for the perchlorate and nitrate are consistent with $\theta(\text{P}-\text{Ag}-\text{P})$ in the solid-state structures already being quite large and able to accommodate changes in the conformational structure of the ligands. The differences in the results for the halide and pseudo-halide complexes imply different behaviours of these two classes of complex in solution but the reasons for this remain speculative at this stage.

Acknowledgements

We acknowledge support of this work by grants from the Australian Research Grants Scheme, the New Zealand University Grants Committee, and the University of Auckland Research Committee. We thank Dr. Sue Berners-Price (Director, Griffith University Magnetic Resonance Facility) for many helpful discussions throughout the course of this study and Ms. Catherine Hobbs for recording the far-IR spectra.

References

- P. F. Barron, J. C. Dyason, P. C. Healy, L. M. Engelhardt, B. W. Skelton and A. H. White, *J. Chem. Soc., Dalton Trans.*, 1986, 1965.
- G. A. Bowmaker, Effendy, J. V. Hanna, P. C. Healy, G. J. Millar, B. W. Skelton and A. H. White, *J. Phys. Chem.*, 1995, **99**, 3909.
- M. I. Bruce, M. L. Williams, B. W. Skelton and A. H. White, *J. Chem. Soc., Dalton Trans.*, 1983, 799.
- C. S. W. Harker and E. R. T. Tiekink, *Acta Crystallogr., Sect. C*, 1989, **45**, 1815.
- W. Lin, T. H. Warren, R. G. Nuzzo and G. S. Girolami, *J. Am. Chem. Soc.*, 1993, **115**, 11 644.
- S. M. Socol, R. A. Jacobson and J. G. Verkade, *Inorg. Chem.*, 1984, **23**, 88.
- E. R. T. Tiekink, *J. Coord. Chem.*, 1988, **17**, 239.
- E. C. Alyea, G. Ferguson and A. Somogyvari, *Inorg. Chem.*, 1982, **21**, 1369.
- A. Baiada, F. H. Jardine and R. D. Willett, *Inorg. Chem.*, 1990, **29**, 3042.
- L.-J. Baker, G. A. Bowmaker, Effendy, B. W. Skelton and A. H. White, *Aust. J. Chem.*, 1992, **45**, 1909.
- M. Camalli and F. Caruso, *Inorg. Chim. Acta*, 1988, **144**, 205.
- G. Wulfsberg, D. Jackson, W. Ilsley, S. Dou and A. Weiss, *Z. Naturforsch., Teil A*, 1992, **47**, 75.
- G. A. Bowmaker, Effendy, J. H. Hanna, P. C. Healy, B. W. Skelton and A. H. White, *J. Chem. Soc., Dalton Trans.*, 1993, 1387.
- A. Cassel, *Acta Crystallogr., Sect. B*, 1979, **35**, 174.
- J. Howatson and B. Morosin, *Cryst. Struct. Commun.*, 1973, **2**, 51.
- P. G. Jones, *Acta Crystallogr., Sect. C*, 1993, **49**, 1148.
- T. Allman and R. G. Goel, *Can. J. Chem.*, 1982, **60**, 716.
- S. R. Hall, H. D. Flack and J. M. Stewart, *The XTAL 3.2 Reference Manual*; Universities of Western Australia, Geneva and Maryland; 1992.
- M. Barrow, H. B. Bürgi, M. Camalli, F. Caruso, E. Fischer, L. M. Venanzi and L. Zambonelli, *Inorg. Chem.*, 1983, **22**, 2356.
- F. Caruso, M. Camalli, H. Rimmi and L. M. Venanzi, *Inorg. Chem.*, 1995, **34**, 673.
- H. B. Bürgi, R. W. Kunz and P. S. Pregosin, *Inorg. Chem.*, 1980, **19**, 3707.
- K. P. Huber and G. Herzberg, *Constants of Diatomic Molecules*, D. van Nostrand, New York, 1979.
- G. A. Bowmaker and P. D. W. Boyd, *J. Mol. Struct. Theochem.*, 1985, **122**, 299.
- G. A. Bowmaker, P. D. W. Boyd and R. J. Sorrenson, *J. Chem. Soc., Faraday Trans. 2*, 1985, **81**, 1627.
- R. D. Ernst, J. W. Freeman, L. Stahl, D. R. Wilson, A. M. Arif, B. Nuber and M. L. Ziegler, *J. Am. Chem. Soc.*, 1995, **117**, 5075.
- P. Gans, J. B. Gill and D. P. Fearnley, *J. Chem. Soc. Dalton Trans.*, 1981, 1708.

- 27 O. H. Ellestad, P. Klæboe, E. E. Tucker and J. Songstad, *Acta Chem. Scand.*, 1972, **26**, 3579.
- 28 T. M. Loehr and T. V. Long, *J. Chem. Phys.*, 1970, **53**, 4182.
- 29 K. Nakamoto, *Infrared and Raman Spectra of Inorganic and Coordination Compounds*, 4th edn., Wiley, New York, 1986.
- 30 G. A. Bowmaker and D. A. Rogers, *J. Chem. Soc., Dalton Trans.*, 1982, 1873.
- 31 P. Braunstein and R. J. H. Clark, *J. Chem. Soc., Dalton Trans.*, 1973, 1845.
- 32 G. A. Bowmaker and R. Whiting, *Aust. J. Chem.*, 1976, **29**, 1407.
- 33 G. A. Bowmaker and D. A. Rogers, *J. Chem. Soc., Dalton Trans.*, 1984, 1249.
- 34 S. Attar, N. W. Alcock, G. A. Bowmaker, J. S. Frye, W. H. Bearden and J. H. Nelson, *Inorg. Chem.*, 1991, **30**, 4166.
- 35 L.-J. Baker, G. A. Bowmaker, D. Camp, Effendy, P. C. Healy, H. Schmidbaur, O. Steigelmann and A. H. White, *Inorg. Chem.*, 1992, **31**, 3656.
- 36 A. Pidcock, R. E. Richards and L. M. Venanzi, *J. Chem. Soc. A*, 1966, 1707.
- 37 J. A. Pople and D. P. Santry, *Mol. Phys.*, 1964, **8**, 1.
- 38 E. L. Muetterties and C. W. Alegranti, *J. Am. Chem. Soc.*, 1972, **94**, 6386.
- 39 E. L. Muetterties and C. W. Alegranti, *J. Am. Chem. Soc.*, 1970, **92**, 4114.
- 40 R. G. Goel and P. Pilon, *Inorg. Chem.*, 1978, **17**, 2876.
- 41 G. A. Bowmaker, Effendy, P. J. Harvey, P. C. Healy, B. W. Skelton and A. H. White, following paper.

Received 15th December 1995; Paper 5/08156D